Ablation of the Retinoblastoma gene family deregulates G$_1$ control causing immortalization and increased cell turnover under growth-restricting conditions

Jan-Hermen Dannenberg, Agnes van Rossum, Leontine Schuijff, and Hein te Riele[1]

The Netherlands Cancer Institute, Division of Molecular Biology, 1066 CX Amsterdam, The Netherlands

The retinoblastoma suppressor pRB belongs to the family of so-called pocket proteins, which also includes p107 and p130. These proteins may functionally overlap in cell cycle control and tumor suppression. We have generated an isogenic set of embryonic stem (ES) cell lines carrying single or compound loss-of-function mutations in the *Rb* gene family, including a cell line completely devoid of all three pocket proteins. None of the knockout combinations affected the growth characteristics of ES cells; however, concomitant ablation of all three pocket proteins strongly impaired their differentiation capacity. For the generated genotypes, primary mouse embryonic fibroblasts (MEFs) also were obtained. While inactivation of *Rb* alone did not alleviate the senescence response of MEFs, pRB/p107-deficient MEFs, after having adapted to in vitro culturing, continued to proliferate at modest rate. Additional ablation of p130 rendered MEFs completely insensitive to senescence-inducing signals and strongly increased their proliferation rate. Although triple-knockout MEFs retained anchorage dependence, they lacked proper G$_1$ control and showed increased cell turnover under growth-inhibiting conditions.

Loss of function of the retinoblastoma suppressor gene, *RB*, is a common event in the development of many tumor types in human, including hereditary retinoblastoma and sporadic lung, breast, and bladder carcinomas (Harbour et al. 1988; Lee et al. 1988; Horowitz et al. 1990). Numerous biochemical studies have placed pRB at the heart of the cellular machinery that controls passage from G$_1$ into S phase of the cell cycle (Weinberg 1995). pRB can exist in hyper- and hypophosphorylated forms, the latter binding to and inhibiting a class of transcription factors, collectively known as E2 factors (E2F), whose activity is required for the transcription of genes that are essential for DNA synthesis (Bernards 1997; Dyson 1998; Nevins 1998). Phosphorylation of pRB by cyclin-dependent kinases (CDK) leads to dissociation of the pRB/E2F complex, releasing the transcriptional activity of E2Fs. CDK activity is positively regulated by heterodimerization with cyclins but also negatively regulated by cyclin-dependent-kinase inhibitors (CKIs). pRB

function can thus be described as a cell cycle switch: cyclin D1-stimulated kinase activity of CDK4 turns pRB -OFF- through phosphorylation; this releases E2F activity and promotes G$_1$-S transition; the pRB -ON- state is favored by inhibition of CDK4 activity by the CKI p16^{INK4A}, which promotes cell cycle arrest. The importance of this G$_1$-S control pathway is underscored by the finding that in the majority of human cancers, genetic alterations have been found that favor the pRB -OFF- state. These include genetic inactivation of *RB* in retinoblastoma and many other cancers; *cyclin D1* overexpression in carcinomas of the breast, oesophagus, and head and neck; *CDK4* amplification or mutational activation in melanomas; and abrogation of *p16^{INK4A}* activity in melanomas, pancreatic, and bladder carcinomas (Hall and Peters 1996; Sherr 1996).

Although the G$_1$-S control pathway described above provided a framework for understanding the tumor-suppressor function of pRB, cell cycle control in mammalian cells is a far more complex circuitry of different, at least partially overlapping and interacting pathways that are regulated by positive and negative feedback mechanisms and can be modulated at numerous levels. Thus, pRB

shares its E2F-regulating activity with two homologs, p107 and p130 (for review, see Mulligan and Jacks 1998; Nevins 1998; Lipinski and Jacks 1999). The three proteins share extensive structural homology, most notably located in two regions, A and B, which together form the so-called pocket domain responsible for binding to E2Fs. These domains also form the binding site for many viral oncoproteins, including adenovirus E1A, simian virus 40 large-T antigen, and human papillomavirus E7, all of which abrogate interactions with E2F (DeCaprio et al. 1988; Whyte et al. 1988; Dyson et al. 1989). Also outside the A/B domain, p107 and p130 share extensive homology, whereas corresponding pRB regions and even the pRB spacer region that separates the A and B subdomains appear to be unique. The closer resemblance between p107 and p130 is underscored by a number of observations suggesting that the two proteins can functionally substitute for each other. p107 and p130 almost exclusively interact with E2F4,5, although they do so at consecutive stages of the cell cycle: Complexes of p130 and E2F4,5 predominate in quiescent or differentiated cells; p107/E2F4,5 complexes are only detected in cycling cells. In contrast, pRb has strongest affinity for E2F1,2,3, although it can also bind E2F4 (for review, see Dyson 1998). Rather than merely sequestering E2Fs, pocket-protein/E2F complexes appear to be actively involved in transcriptional repression (Zhang et al. 1999). While no differences in expression of E2F target genes were found on ablation of p107 or p130 alone, combined loss in $p107^{-/-}p130^{-/-}$ primary mouse embryonic fibroblasts (MEFs) resulted in derepression of a number of genes, including *B-myb*, *Cdc2*, *E2f1*, *Ts*, *Rrm2*, and *Cyclin A2*. Expression of these genes was normal in $Rb^{-/-}$ MEFs, but in these cells, *Cyclin E* and *p107* were slightly up-regulated (Herrera et al. 1996; Hurford et al. 1997). Thus, p107 and p130 appeared to be redundant in regulating a specific set of E2F-responsive genes that is not subject to pRb/E2F-mediated repression. However, overexpression of each of the pocket proteins in vitro can cause cell cycle arrest, an activity that can be relieved through phosphorylation by cyclinD/CDK4,6. Full inactivation of pRB also requires cyclinE/CDK2, which adds an additional level of regulation to the pRB pathway. Thus, the three pocket proteins may to some extent be redundant in blocking progression of cells through the cell cycle. In resting T lymphocytes, the main pocket protein/E2F complex is p130/E2F4. However, in the absence of p130, E2F4 was mainly found complexed to p107 or, when this protein was also absent, to pRb (Mulligan et al. 1998). Apparently, in this system pocket proteins can compensate for each other in regulating E2F4 activity, providing a rationale for their shared activities in blocking cell cycle progression.

Specific and redundant functions of pocket proteins also became manifest in mice carrying single or compound disruptions in the *Rb* gene family (Mulligan and Jacks 1998). Complete inactivation of *Rb* appeared not to be compatible with normal development (Clarke et al. 1992; Jacks et al. 1992; Lee et al. 1992). $Rb^{-/-}$ embryos died at midgestation, presenting with extensive apopto-sis in the central nervous system and eye lens and defects in erythropoiesis and myogenesis. These defects could at least partially be attributed to increased free E2F1 activity, inducing p53-dependent apoptosis (Morgenbesser et al. 1994; Tsai et al. 1998). In contrast, genetic ablation of either *p107* or *p130* did not show an overt phenotype (Cobrinik et al. 1996; Lee et al. 1996). However, combination of *p107* and *p130* loss-of-function mutations caused excessive chondrocyte proliferation leading to malformation of the long bones and ribs. Respiratory problems associated with this defect led to rapid neonatal death. Remarkably, a dramatic phenotype was observed when loss-of-function mutations in either *p107* or *p130* were crossed into the BALB/c background (Le-Couter et al. 1998a,b): p107 deficiency caused impaired growth of newborns, while embryonic fibroblasts displayed a twofold reduction in doubling time; p130-deficient embryos died at midgestation and showed marked apoptosis in the central nervous system. BALB/c mice were found to carry a point mutation in the $p16^{Ink4a}$ gene (Zhang et al. 1998). These observations suggest that p107 and p130 can functionally substitute for each other, but only in the presence of a pathway that requires wild-type p16 and most likely involves pRB. Conversely, p107 appeared to attenuate the consequences of pRB deficiency in development as p107/pRB-deficient embryos showed a reduced life span with respect to embryos lacking only pRB (Lee et al. 1996). p107 activity also appeared to modulate the tumor suppressor function of pRB. In contrast to humans, where hemizygosity for the retinoblastoma suppressor gene *RB* highly predisposes to retinoblastoma, $Rb^{+/-}$ mice developed tumors originating from the intermediate lobe of the pituitary gland while the retina remained unaffected (Hu et al. 1994; Robanus-Maandag et al. 1994). No predisposition to tumorigenesis was found to be associated with p107 or p130 deficiency (Cobrinik et al. 1996; Lee et al. 1996). However, concomitant inactivation of *Rb* and *p107* in chimeric mice gave rise to retinoblastoma development, indicating that p107 can act as a tumor suppressor in the context of pRb deficiency (Robanus-Maandag et al. 1998).

Primary mouse embryonic fibroblasts represent a rather well-defined cell type that has been widely used to identify the consequences of gene ablation for cell cycle control. Although pRB deficiency or combined p107/p130 deficiency caused a slight acceleration of S-phase entry on restimulation of serum-starved cells, the overall growth characteristics of single- or double-knockout MEFs did not deviate from those of wild-type MEFs (Cobrinik et al. 1996; Herrera et al. 1996). In particular, the single- and double-knockout genotypes tested thus far did not affect the growth arrest response of cells to a number of growth-inhibiting conditions such as serum deprivation, contact inhibition, and prolonged passaging. This again suggests functional redundancy within the pocket-protein family. To test this directly, we have now generated MEFs that are completely devoid of all three pocket proteins. Our results identify the pocket proteins as critical mediators of senescence and of the response of cells to a variety of growth-restricting conditions.

Results

Inactivation of Rb, p107, and p130 in ES cells

An isogenic set of wild-type (*wt*), *Rb*$^{-/-}$, *Rb*$^{-/-}$*p107*$^{-/-}$, and *Rb*$^{-/-}$*p107*$^{-/-}$*p130*$^{-/-}$ embryonic stem (ES) cell lines was generated by consecutive rounds of homologous recombination. The generation of *Rb*$^{-/-}$ and *Rb*$^{-/-}$*p107*$^{-/-}$ ES cell lines has been described before (Te Riele et al. 1992; Robanus-Maandag et al. 1998). To inactivate *p130*, we generated a 129p130-pur targeting vector (Fig. 1A). *Rb*$^{-/-}$*p107*$^{-/-}$*p130*$^{-/-}$ cells were obtained in two ways: First, *p130* was inactivated in *Rb*$^{-/-}$*p107*$^{-/-}$ ES cells and *Rb*$^{-/-}$*p107*$^{-/-}$*p130*$^{+/-}$ cells were cultured at high puromycin concentrations to select for inactivation of the remaining *p130* wild-type allele; second, both *p130* alleles were inactivated in *p107*$^{-/-}$ ES cells and then *Rb* was inactivated using the targeting vectors 129Rb-hyg and 129Rb-his. Figure 1B shows that p130 protein was not detectable in brain tissue obtained from a *p130*$^{-/-}$ mouse carrying the same disruption in *p130*, indicating that the *p130*$^-$ allele can be considered a null allele. Thus, *Rb*$^{-/-}$*p107*$^{-/-}$*p130*$^{-/-}$ cells are completely devoid of pocket proteins and will hereafter be designated as triple-knockout (*TKO*) cells. Each genotype was derived in duplicate by

independent rounds of gene targeting starting from wild-type cells. None of the generated genotypes in ES cells resulted in an obvious phenotype, indicating that the pocket proteins pRB, p107, and p130 are dispensable for normal ES cell growth.

Limited differentiation capacity of Rb$^{-/-}$p107$^{-/-}$p130$^{-/-}$ ES cells in teratocarcinomas

To study whether pocket proteins become essential during differentiation of ES cells, we injected *wt*, *Rb*$^{-/-}$, *Rb*$^{-/-}$*p107*$^{-/-}$, and *Rb*$^{-/-}$*p107*$^{-/-}$*p130*$^{-/-}$ ES cells subcutaneously into nude mice. In this environment, ES cells form teratocarcinoma-like tumors in which a variety of differentiated cell types can be identified, including neuronal and muscle cells. Three weeks after injection the teratocarcinomas were removed and histologically examined. Tumors derived from *wt*, *Rb*$^{-/-}$, and *Rb*$^{-/}$$_{-}$*p107*$^{-/-}$ ES cells were highly similar with respect to their strongly heterogeneous appearance with extensive neuronal differentiation (Fig. 2A) and striated muscle (Fig. 2B). Extensive neuronal differentiation was confirmed by staining with the neuron-specific antibodies
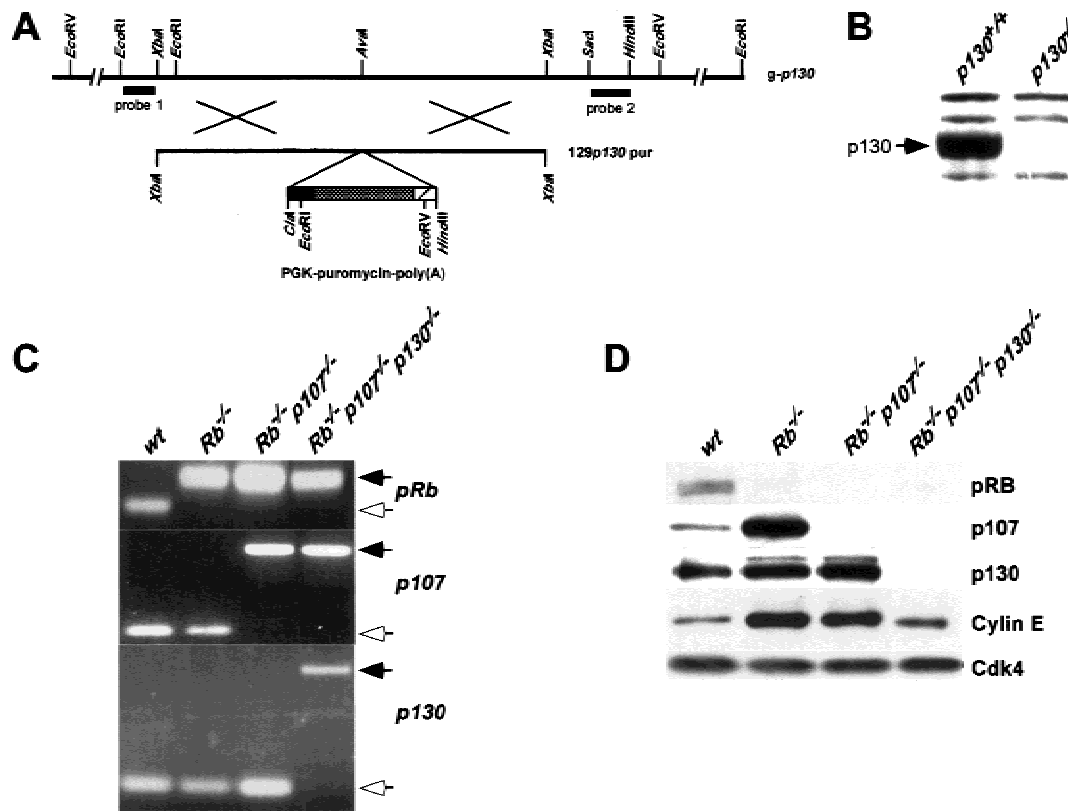
Figure 1. Generation of *Rb*$^{-/-}$*p107*$^{-/-}$*p130*$^{-/-}$ ES cells and MEFs. (*A*) Restriction map of the wild-type *p130* allele around codon 405 at the *Ava*I site and 129*p130*-pur DNA targeting construct. Probes 1 and 2 detect modifications at *p130*. (*B*) Western blot analysis of p130 in lysates prepared from *p130*$^{+/+}$ and *p130*$^{-/-}$ brain tissue. (*C*) PCR analysis of *Rb*, *p107* and *p130* of DNA isolated from passage 1 *wt*, *Rb*$^{-/-}$, *Rb*$^{-/-}$*p107*$^{-/-}$ and *TKO* MEFs. PCR products resulting from wild-type and knockout alleles of each gene are indicated by open and solid arrows, respectively. (*D*) Western blot analysis of pRB, p107, p130, and Cyclin E in lysates prepared from indicated MEFs. Cdk4 served as a loading control.
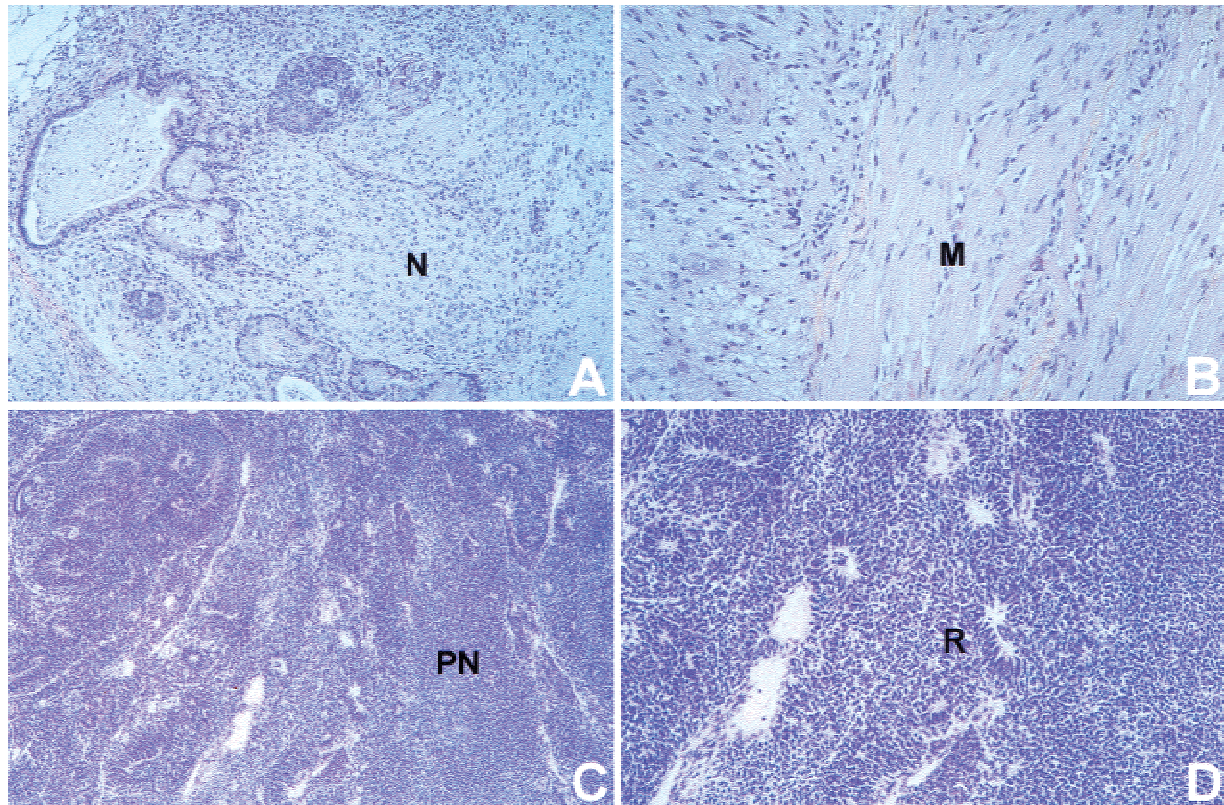
Figure 2. Limited differentiation in *TKO* teratocarcinomas. Histological sections of teratocarcinomas were stained with hematoxylin-eosin. (*A,B*) Advanced neuronal (N) and muscle (M) differentiation in teratocarcinomas generated with *wt* ES cells. Similar results were obtained with $Rb^{-/-}$ and $Rb^{-/-}p107^{-/-}$ ES cells. (*C,D*) Cell-dense *TKO* teratocarcinomas lack muscle differentiation and exist of primitive, relatively undifferentiated neuronal cells (PN) with rosette-like structures (R). Magnification (*A,C*) objective 10×, (*B,D*) objective 20×.

anti-glial fibrillary acidic protein (GFAP) and anti-neuron specific enolase (NSE; not shown). In contrast, *TKO* ES cells formed a rather homogeneous tumor mass, without any muscle cell differentiation (Fig. 2C). Rosette-like structures and positive staining with a p75^{LNGFR} antibody (Zorick and Lemke 1996) indicated that *TKO* tumors predominantly consisted of neuroblast-like cells (Fig. 2D; not shown). Furthermore, immunohistochemistry using antibodies directed against the proliferation marker Ki-67 showed that the fraction of proliferating cells in *TKO* tumors was 15-fold higher than in teratocarcinomas of the other genotypes. These data show that in this system, ablation of the *Rb* gene family abrogates neuronal and muscular differentiation.
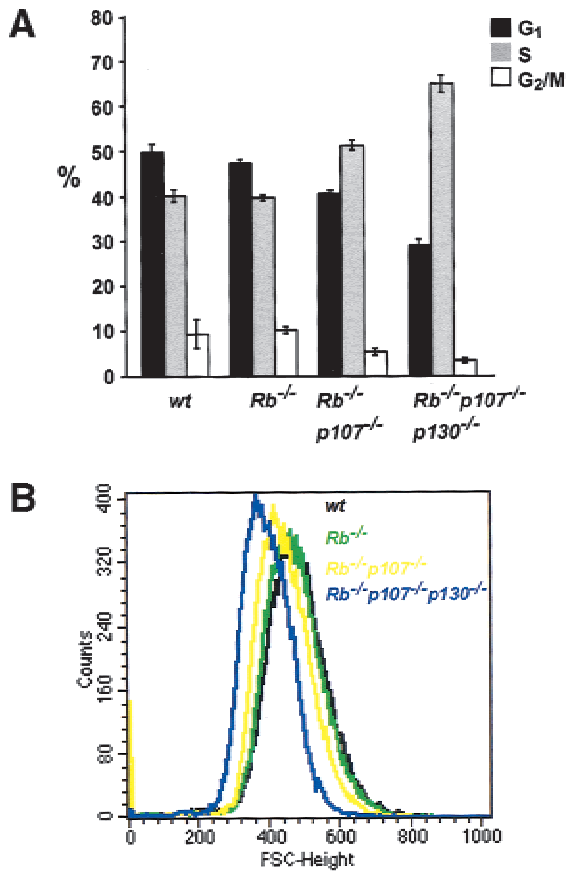
Pocket-protein-deficient MEFs obtained from chimeric embryos

Primary MEFs have been instrumental in studying the consequences of gene ablation for cell cycle control. We have derived an isogenic set of MEFs from chimeric embryos generated by blastocyst injections of mutant ES cells. In these experiments, we used ES cells that also contained a neomycin resistance gene under the control of the *Rosa26* promoter (Friedrich and Soriano 1991; J.-H.

Dannenberg and H. te Riele, in prep.). Brief culturing in the presence of G418 provided a uniform method to obtain MEF preparations that were exclusively ES-cell derived. This was verified by genotyping these cells by PCR for the presence of the wild-type and knockout alleles of *Rb*, *p107*, and *p130* (Fig. 1C). The presence or absence of pocket proteins was further confirmed by Western blot analyses (Fig. 1D). We were able to generate MEF cultures with the following genotypes: *wt*, $Rb^{-/-}$, $Rb^{-/-}p107^{-/-}$, and somewhat surprisingly, $Rb^{-/-}p107^{-/-}p130^{-/-}$.

Pocket proteins are essential for G_1 control

Proliferating MEF cultures of early passage were labeled with the thymidine analogue BrdU and analyzed by FACS. Figure 3A shows that concomitant inactivation of *Rb*, *p107*, and *p130* strongly reduced the percentage of cells in G_1. This decrease in G_1 fraction was accompanied by an increase of the S-phase population, with *TKO* MEF cultures having up to 65% S-phase cells. In $Rb^{-/-}$ MEFs, only a minor decrease in G_1 population was observed, whereas disruption of both *Rb* and *p107* gave an intermediate phenotype. Together with the strongly reduced population-doubling time of *TKO* cells (see below; Fig. 4), these observations suggest that successive abla-

Figure 3. Deregulated G$_1$-control in *TKO* MEFs. (*A*) Percentages of G$_1$, S, and G$_2$/M phases of the cell cycle in proliferating wild-type (*wt*) and pocket-protein-deficient MEFs. Results are indicated as average values of three independent experiments. Error bars indicate standard deviations of the mean. (*B*) FSC-H histogram showing cell-size analysis of MEFs deficient for *Rb*, *p107*, and *p130* compared with *wt* counterparts. The forward scatter, FSC-H, is indicative for the cell diameter, and a shift to the left, relative to the *wt* MEFs, represents smaller cells.

tion of pRb, p107, and p130 reduces the length of the G$_1$ phase of the cell cycle.

   G$_1$ shortening has previously been correlated to a decrease in cell size in several other experimental settings, such as overexpression of cyclin E (Ohtsubo and Roberts 1993) and concomitant inactivation of *Rb* and *p21* (Brugarolas et al. 1998). We therefore determined the size of wild-type and mutant MEFs. Proliferating cultures of early passage were fixed, stained with propidiumiodide (PI), and analyzed by FACS (Fig. 3B). Relative cell sizes closely correlated to the proportion of cells in G$_1$: *TKO<Rb$^{-/-}$p107$^{-/-}$<Rb$^{-/-}$ = wt*. This again indicates that ablation of pocket proteins reduces the length of G$_1$.

   It is of interest to note that in cyclin-E-overexpressing or *Rb/p21*-deficient cells, G$_1$ shortening has been correlated with increased cyclin E levels or elevated CDK2 kinase activity. However, whereas *Rb$^{-/-}$* and *Rb$^{-/-}$ p107$^{-/-}$* MEFs showed increased levels of cyclin E, *TKO* MEFs expressed cyclin E at wild-type levels (Fig. 1D).

Thus, shortening of G$_1$ is not obligatorily accompanied by elevated levels of cyclin E.

Rb$^{-/-}$p107$^{-/-}$p130$^{-/-}$ *MEFs are immortal*

Wild-type MEFs have a limited growth capacity on prolonged passaging: Their growth rate gradually decreases until they finally completely arrest with an enlarged, flattened morphologoly and 2n DNA content, a state that is referred to as replicative senescence (Todaro and Green 1963; Campisi 1997). The involvement of the *Rb* gene family in senescence was assessed in two ways.
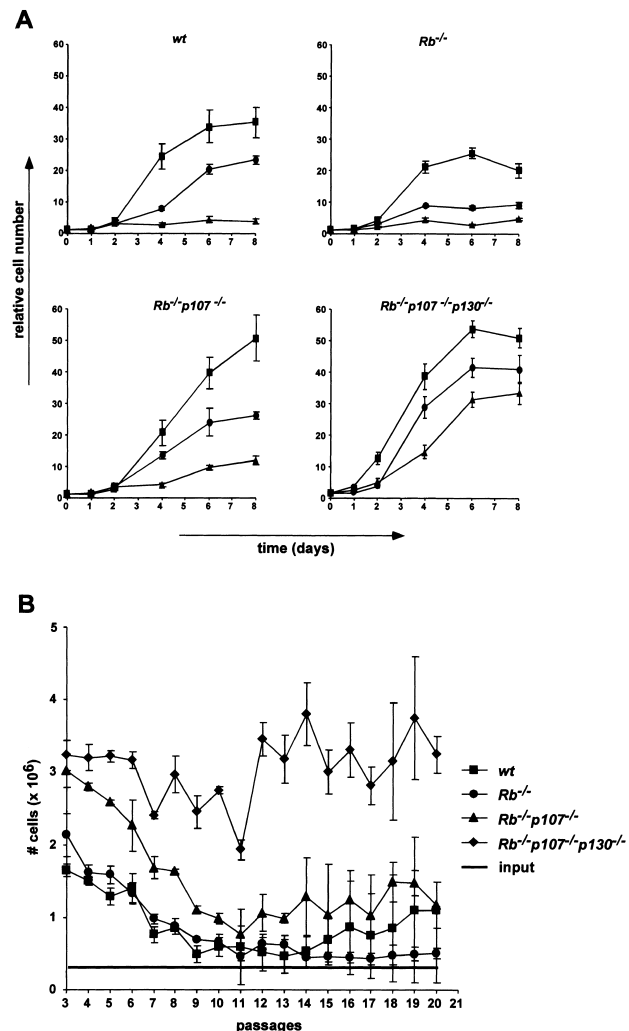

Figure 4. Growth characteristics of pocket-protein-deficient MEFs. (*A*) Growth curves of *wt*, *Rb$^{-/-}$*, *Rb$^{-/-}$p107$^{-/-}$*, and *TKO* MEFs at passages 3 (squares), 5 (circles), and 7 (triangles). The figure shows a representative of three independent experiments, each performed in triplicate. (*B*) Cell proliferation on a 3T9-based protocol of indicated MEFs for 20 passages. At 3.5-d intervals, the total numbers of cells of three independent cultures of each genotype were determined before redilution of the cells to 3×10^5 per six-well plate (input). The experiment was performed twice. Error bars indicate standard deviations of the mean.

First, we determined the growth rates of *wt*, *Rb*$^{-/-}$, *Rb*$^{-/-}$
p107$^{-/-}$, and *TKO* MEFs at increasing passages. Figure 4A
shows that the growth rates of *wt* and *Rb*$^{-/-}$ MEFs gradu-
ally decreased on prolonged passaging and that these
cells entered senescence around passage seven. *Rb*$^{-/-}$
p107$^{-/-}$ MEFs showed a fivefold reduction in growth
rate; however, they had not completely ceased prolifer-
ating at passage seven (Fig. 4A) and clearly had not
adopted a senescence-like morphology (not shown). *TKO*
MEFs retained the strongest proliferative capacity at
later passages, their growth rate being reduced less than
twofold. Second, the long-term proliferative capacity of
MEFs was assessed following a 3T9-based protocol (Fig.
4B). Wild-type, *Rb*$^{-/-}$, and *Rb*$^{-/-}$*p107*$^{-/-}$ MEFs showed a
decline in proliferation rate up to passage 11. While the
Rb$^{-/-}$ cells completely stopped growing in this experi-
ment, *wt* cells ultimately escaped from senescence as a
result of a genetic alteration (see also below). *Rb*$^{-/-}$
p107$^{-/-}$ MEFs, although initially subject to growth inhi-
bition, did not enter senescence but established a con-
stant proliferation rate of one to two population dou-
blings every 3 d. Also, *TKO* cells initially showed some
decline in growth rate. However, this decline was mar-
ginal, and the cells continued to proliferate at a rate that
was about threefold higher than the double knockouts.
These results demonstrate that inactivation of *Rb* alone

does not alleviate the senescence response of MEFs; con-
comitant inactivation of *Rb* and *p107*, although not com-
pletely alleviating growth inhibition on in vitro cultur-
ing, confers a continuing proliferation capacity, albeit at
a modest rate, whereas ablation of all *Rb*-gene family
members renders cells virtually insensitive to growth
inhibition on in vitro culturing and strongly increases
their proliferation rate.

Immortal TKO *MEFs retain an intact p19*^{ARF}*/p53 pathway*

It has previously been hypothesized that replicative se-
nescence results from the p53-dependent growth inhibi-
tory effect of p19^{ARF}, which gradually accumulates on
prolonged passaging (Quelle et al. 1995; Zindy et al.
1997). Thus, inactivation of *Ink4a*, *p19*^{Arf}, or *p53* has
been shown to result in immortalization of MEFs (Ser-
rano et al. 1996, 1997; Kamijo et al. 1997). Furthermore,
spontaneous immortalization of MEFs was accompanied
by either mutation of *p53* (Harvey and Levine 1991; Rit-
tling and Denhardt 1992) or deletion of the *Ink4a* locus
(Kamb et al. 1994; Nobori et al. 1994; Zindy et al. 1998),
ablating both p16^{INK4A} and p19^{ARF} (Kamijo et al. 1997).
We therefore tested the functionality of this pathway in
immortal *TKO* MEFs. Figure 5A shows that *p16*^{Ink4a}
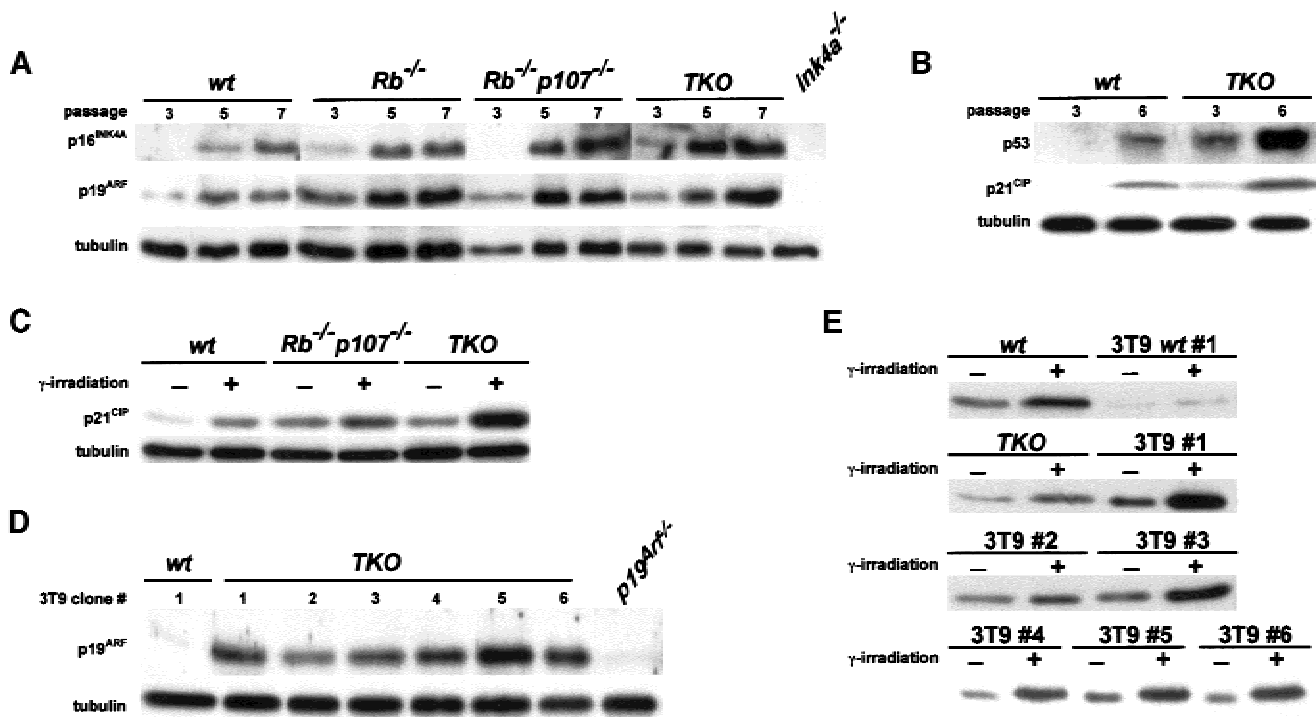
Figure 5. Intact p19^{ARF}/p53 pathway in immortal *TKO* MEFs. (*A*) Indicated MEFs were passaged according to a 3T9 protocol, and cell
pellets were collected at passages 3, 5, and 7. Cell lysates were analyzed for p16^{INK4A}, p19^{ARF} and tubulin levels by immunoblotting.
Ink4a$^{-/-}$ MEFs served as a negative control. (*B*) Expression of p53 and p21^{CIP} in *wt* and *TKO* MEFs at passages 3 and 6. (*C*) Expression
analysis of p21^{CIP} in control and γ-irradiated early passage *wt*, *Rb*$^{-/-}$*p107*$^{-/-}$ and *TKO* MEFs showing induction of *p21*^{Cip} in all
genotypes 24 h after irradiation. (*D*) Expression analysis of p19^{ARF} in six independent *TKO* 3T9 clones (1–6). All clones expressed
p19^{Arf}, whereas a wild-type 3T9 clone (3T9*wt*, 1) had lost expression of this protein. *p19*$^{Arf-/-}$ MEFs served as a negative control. (*E*)
Induction of *p21*^{Cip} in γ-irradiated *wt* (1) and *TKO* (1–6) 3T9 MEF cell lines compared to γ-irradiated early passage *wt* and *TKO* MEFs.

and $p19^{Arf}$ were properly expressed in all genotypes including *TKO* and tended to increase on prolonged passaging. Also, p53 function was induced as evidenced by increased protein levels and accumulation of p21^{CIP} (Fig. 5B). Furthermore, when *TKO* MEFs were γ irradiated, they showed a strong induction of *p21^{Cip}*, as in *wt* and *Rb$^{-/-}$p107$^{-/-}$* MEFs, again indicating that the cells contained functional p53 (Fig. 5C). These observations indicate that complete loss of function of the *Rb* gene family renders MEFs resistant toward p19^{ARF}/p53-induced senescence and predicts that *TKO* MEFs at passage numbers where wild-type MEFs spontaneously escape from senescence can grow without mutations in *p53* or deletions of the *Ink4a* locus. Indeed, we found that in six independent clones that were grown on a 3T9-based protocol for >20 passages, p19^{ARF} was still expressed, in contrast to a *wt* 3T9 clone that had lost p19^{ARF} expression, probably because of a deletion of the *Ink4a* locus (Fig. 5D). Finally, all six *TKO* 3T9 clones showed increased *p21^{Cip}* expression on γ irradiation, as in *wt* and *TKO*

MEFs of early passage, indicating that p53 also remained functional in these clones (Fig. 5E).

p53 can induce both a pRB-dependent G$_1$ and a pRB-independent G$_2$/M arrest on γ irradiation (Agarwal et al. 1995; Brugarolas et al. 1995; Harrington et al. 1998). Figure 6A shows that a γ-irradiation-induced G$_1$ arrest was indeed abrogated in *Rb$^{-/-}$p107$^{-/-}$* and *TKO* MEFs, while the G$_2$/M checkpoint was still intact. This again indicates that in *Rb$^{-/-}$p107$^{-/-}$* and *TKO* cells, p53 remained functional and that pocket proteins are dispensable for radiation-induced G$_2$/M arrest.

Finally, we asked whether MEFs deficient for the *Rb*-gene family are still sensitive to G$_1$ arrest following ectopic expression of p19^{ARF}. Cells were electroporated and analyzed by FACS. First, we found that introduction of a CDK2 dominant-negative protein increased the G$_1$ population to the same extent in *Rb$^{-/-}$*, *Rb$^{-/-}$p107$^{-/-}$*, and *TKO* MEFs (Fig. 6B). Ectopic expression of p19^{ARF} induced a similar G$_1$ arrest in cells lacking pRB or both pRB and p107. In contrast, in *TKO* MEFs, G$_1$ arrest was
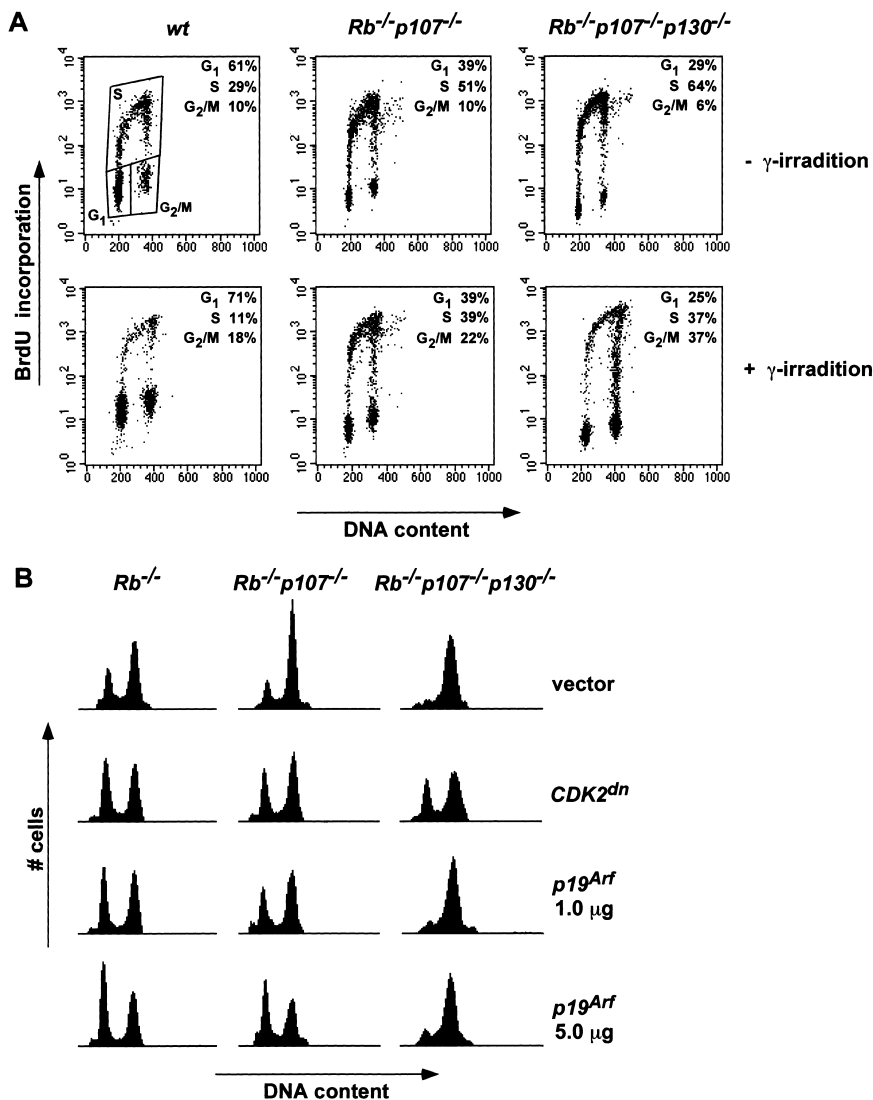
Figure 6. Defective G$_1$ checkpoint in *TKO* MEFs on irradiation and ectopic *p19^{Arf}* expression. (*A*) γ-irradiation induced a G$_2$/M arrest in *Rb$^{-/-}$p107$^{-/-}$* and *TKO* MEFs. Percentages of G$_1$, S, and G$_2$/M phases of the cell cycle in nonirradiated and irradiated (5.5 Gy) MEFs were measured by FITC-PI FACS analysis and plotted as FL3-A (*X*-axis)–FL1-H (*Y*-axis) dot plots. (*B*) Ectopic expression of *p19^{Arf}* induces a pocket-protein-dependent G$_1$ arrest. FACS analysis of GFP-positive *Rb$^{-/-}$*, *Rb$^{-/-}$p107$^{-/-}$* and *TKO* MEFs expressing either vector plasmid, a dominant-negative variant of CDK2, or *p19^{Arf}* (1.0 or 5.0 µg) together with a histone H2B-GFP expression construct in a 10 : 1 ratio. Representative results of three independent experiments are shown.

only marginally induced by $p19^{ARF}$ compared to the effect of $CDK2^{dn}$ (Fig. 6B). Together with the observation that ablation of the *Rb* gene family causes immortalization despite normal levels of INK4A proteins and functional p53, this result indicates that pocket proteins are essential mediators of the senescence response to $p19^{ARF}$.

Inactivation of pocket proteins leads to increased cell turnover under growth-inhibiting conditions

TKO cells are largely refractory to growth inhibition by $p19^{ARF}$. We therefore examined the behavior of these cells under a number of other growth-inhibiting conditions.

Growth factor depletion MEFs were plated at low density, supplied with 0.1% serum, and analyzed by BrdU-FACS. Wt and $Rb^{-/-}$ cells strongly arrested as evidenced by the accumulation of cells in G_1 and a block in DNA synthesis (Fig. 7A). The response of $Rb^{-/-}p107^{-/-}$ MEFs was less pronounced, although the level of DNA synthesis was still significantly decreased compared to 10% serum (see also Fig. 3A). In contrast, *TKO* MEFs continued to incorporate BrdU almost at the same rate as under high serum conditions. Suprisingly, under these conditions, no increase in cell number was observed on prolonged culturing (Fig. 7B). The appearance of floating

cells in the medium at 24 h after the application of low serum suggested that cells became apoptotic. Indeed, PI-FACS analysis revealed a significant sub-G_1 population in *TKO* MEFs at 24 h after low serum addition, increasing up to 10% of the population after 4 d (Fig. 7C). Again, $Rb^{-/-}p107^{-/-}$ showed an intermediate phenotype. We did not observe an increased population of multinucleated MEFs, indicating that continuous BrdU incorporation did not result from endoreduplication (data not shown).

Contact inhibition Another extracellular signal that provokes a G_0/G_1 arrest in normal fibroblasts is cell–cell contact at confluency (Nilausen and Green 1965). This phenomenon, known as contact inhibition, was shown to be accompanied by increased $p27^{KIP1}$ and decreased cyclin D1 levels (Polyak et al. 1994; St. Croix et al. 1998). Furthermore, hypophosphorylated isoforms of pRb accumulated, suggesting that pRB is essential for G_1 arrest. To study the role of pocket proteins in contact inhibition, MEFs were grown to confluency and cultured for an additional 4 d. DNA synthesis was measured by BrdU-FACS. Again, deletion of all pocket proteins revealed a severe defect in establishing a G_0/G_1 arrest (Fig. 7D). Instead, *TKO* MEFs continued to incorporate BrdU and to generate apoptotic cells (Fig. 7E).

Nonadherent conditions Anchorage independance is a characteristic of most oncogenically transformed cell
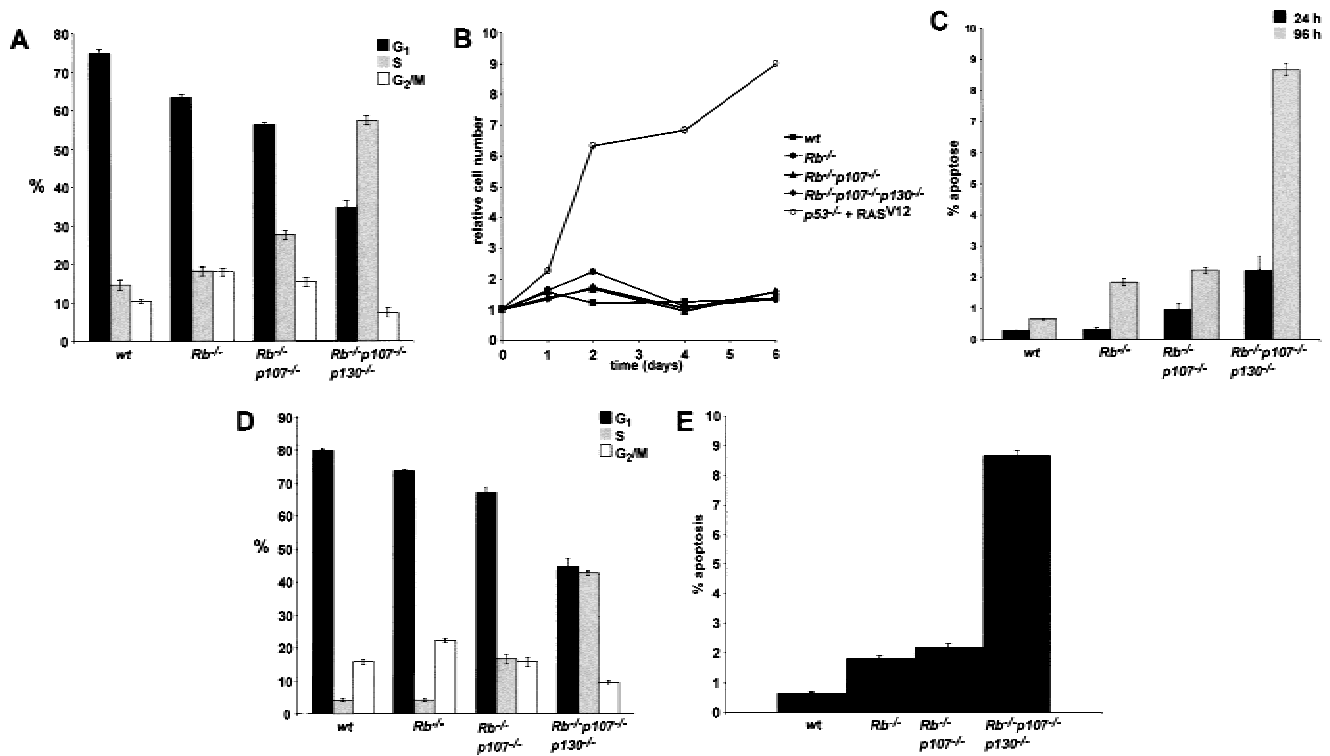
Figure 7. Increased cell turnover in *TKO* MEFs under growth-inhibiting conditions. (*A*) Distribution of G_1, S, and G_2/M phases of indicated MEFs at 0.1% FCS. (*B*) Growth curves of indicated MEFs at 0.1% FCS. (*C*) Percentage of apoptotic cells in indicated MEF cultures at 0.1% FCS, 24 h (black), and 96 h (grey) after growth-factor depletion. Percentages were obtained by determing the sub-G_1 population in a FL3A-log histogram. (*D*) Distribution of G_1, S, and G_2/M phases of indicated contact-inhibited MEFs. (*E*) Percentage apoptotic cells in contact-inhibited MEF cultures. Average values of three independent experiments are indicated in percentages. Error bars indicate standard deviations from the mean (*A,C,D,E*).

types and was attributed to constitutive cyclin E- (Fang et al. 1996) or A- (Guadagno et al. 1993) dependent CDK2 activity. In nonmalignant cells, growth arrest under nonadherent conditions was associated with loss of cyclin E-CDK2 activity (Fang et al. 1996) and underphosphorylation of pRB and p107 (Schulze et al. 1996). However, we found that *TKO* MEFs, although giving very tiny colonies containing up to 20 cells, were not capable of sustained proliferation in soft agar (Table 1). This indicates that ablation of pocket-protein activity is not sufficient for growth under nonadherent conditions and suggests that loss of CDK2 activity can confer a pocket-protein-independent growth arrest. This view is consistent with our observation that *TKO* cells can still be blocked by ablation of CDK2 activity (Fig. 6B). The anchorage dependence of *TKO* MEFs is consistent with their inability to grow under the skin of nude mice (not shown), demonstrating that these cells are not transformed.

In conclusion, complete ablation of the *Rb* gene family does not allow anchorage-independent growth; however, it severely compromises cell cycle arrest in response to growth-factor depletion and contact inhibition. Under these growth-inhibiting conditions, pocket-protein-deficient cells undergo increased cell turnover.

Discussion

We have generated an ES cell line carrying inactivating disruptions in all three retinoblastoma gene family members and found that this strongly limited their differentiating capacity. In MEFs, complete ablation of the pocket-protein family severely compromised G$_1$ control. This was most strikingly manifested by the finding that triple-knockout MEFs were immortal and sustained continuous proliferation and apoptosis under growth-restricting conditions.

Differentiation

ES cells have a very high proliferation rate (doubling time of 7–8 h), and in a proliferating population, ~70% of the cells were found in S phase (Savatier et al. 1994). Savatier et al. (1996) made the surprising observation that undifferentiated ES cells do not contain detectable cyclin D1/CDK4 activity and are insensitive to growth inhibition by p16^{INK4A}. Furthermore, ES cells do not ex-

press p130 (LeCouter et al. 1996), whereas pRB and p107 could be readily detected (Robanus-Maandag et al. 1998). Apparently, in ES cells the antiproliferative effects of pRB and p107 are neutralized, possibly by the presence of an E1A-like activity (E1A-LA), as was postulated before (Murray et al. 1991). The dramatic increase in cyclin D1/CDK4 activity on induction of differentiation likely reflects the pRB/p107/p130 control pathways becoming active. Our observations are fully consistent with this view: Ablation of the pRB family did not affect the growth potential of ES cells but severely compromised their differentiating potential. Thus, pocket proteins are required for differentiation of ES cells. Moreover, as both pRB/p107-deficient ES cells (this work) and p130-deficient ES cells (not shown) showed normal muscular and neuronal differentiation in teratocarcinomas, p130 can compensate for the absence of pRB and p107.

Despite their limited differentiation capacity when placed under the skin of nude mice, *TKO* ES cells injected into blastocysts did not show unrestricted proliferaton but, instead, were capable of contributing to embryonic development at least until day 15 of gestation, allowing the derivation of *TKO* MEFs. This observation may suggest that differentiation into certain cell types, for example, fibroblasts, does not require pocket-protein function. More intriguing is the possibility that differentiation of *TKO* cells in chimeric embryos is directed and controlled by surrounding wild-type cells. In either case, during development, the cells have apparently acquired characteristics that, unlike their embryonic stem cell progenitors, prevent them from growing anchorage independently or under the skin of nude mice.

Immortalization

In both human and mouse primary fibroblasts, prolonged culturing generates a growth-inhibiting signal that ultimately leads to a state of replicative senescence reflected by an enlarged, flattened morphology and the absence of DNA synthesis (Hayflick and Moorhead 1961; Todaro and Green 1963; Campisi 1997). This type of growth arrest is accompanied by gradually increasing levels of the CDK2/4 inhibitors, p21^{CIP} and p16^{INK4A}, the cell cycle inhibitor p19^{ARF}, and p53 (Lloyd et al. 1997; Palmero et al. 1997; Zindy et al. 1997, 1998). p16^{INK4A} and p19^{ARF} are encoded by one genetic locus, *Ink4a*, whereby p19^{ARF} is expressed from an alternative reading frame (Quelle et al. 1995). Whereas p16^{INK4A} was shown to act upstream of pRB to promote cell cycle arrest (Serrano et al. 1993), p19^{ARF} can physically interact with p53 and/or MDM2, thereby antagonizing the function of MDM2 and stabilizing p53 (Kamijo et al. 1998; Pomerantz et al. 1998; Zhang et al. 1998). Spontaneous immortalization of MEFs is usually accompanied by either deletion of the *Ink4a* locus (Kamb et al. 1994; Nobori et al. 1994; Kamijo et al. 1997; Zindy et al. 1998) or loss of p53 function (Harvey and Levine 1991; Rittling and Denhardt 1992). Furthermore, *Ink4a*$^{-/-}$ and *p53*$^{-/-}$ MEFs are immortal. These observations suggest that induction of INK4A proteins and p53 is causally related to induction of senes-

Table 1. *Immortal TKO MEFs do not grow anchorage independently*

Genotype MEFs	Exp I	Exp II	Exp III
wt	0	0	0
Rb$^{-/-}$	0	0	0
RB$^{-/-}$*p107*$^{-/-}$	0	0	0
Rb$^{-/-}$*p107*$^{-/-}$*p130*$^{-/-}$	0^a	0	0
p53$^{-/-}$ + RAS^{V12}	229	238	273

Number of foci of indicated early passage MEFs appearing after 2 wk in soft agar.

[a]A small percentage of the MEFs developed into tiny colonies (up to 20 cells) but did not sustain growth.

cence. However, mice and MEFs lacking only p19^{ARF} showed a phenotype indistinguishable from that resulting from disruption of the *Ink4a* locus abrogating both p16^{INK4A} and p19^{ARF}. Although the consequences of ablation of p16^{INK4A} alone are unknown, this suggests that the p19^{ARF}/p53 rather than the p16^{INK4A}/pRB pathway is responsible for inducing senescence.

We now show that MEFs deficient for pRB, p107, and p130 are immortal, cannot be arrested by ectopic p19^{ARF} expression, and do not sustain deletions of the *Ink4a* locus or mutations in *p53* on prolonged passaging. Also, pRB/p107-deficient MEFs can be considered immortal: Although they respond to supraphysiological levels of p19^{ARF} by a G$_1$ arrest, after having adapted to in vitro culturing, they sustained a moderate but constant proliferation rate on prolonged passaging. These observations indicate that both p19^{ARF}-induced senescence and cell cycle arrest require pRB family members. It therefore remains plausible that both products of the *Ink4a* locus are implicated in senescence induction, p16^{INK4A} not being sufficient but facilitating the activation of pocket proteins by p19^{ARF} (Carnero et al. 2000). How p19^{ARF} signals to the pRB family remains unclear. The immortal phenotype of *p53*$^{-/-}$ MEFs suggests this pathway to be p53 dependent. However, p19^{ARF}-p53-induced senescence is not implemented via p21^{CIP}-induced inhibition of cyclin E/CDK2, as *p21*$^{-/-}$ and *p21*$^{-/-}$*p27*$^{-/-}$ MEFs still undergo senescence and/or are responsive to overexpression of p19^{ARF} (Pantoja and Serrano 1999; Groth et al. 2000). Furthermore, our data show that *TKO* MEFs are not blocked in G$_1$ by p19^{ARF} overexpression, although they can still be blocked by inhibition of CDK2 activity on expression of a dominant-negatively acting CDK2 mutant. A picture thus emerges wherein p19^{ARF} induces senescence via the pRB family but independent of p21^{CIP}-mediated inhibition of cyclin E/CDK2 activity. Whether the link between p19^{ARF} and the *Rb* gene family is p53 dependent remains obscure. In contrast to one report (Kamijo et al. 1997), another showed that p19^{ARF} could induce a cell cycle arrest in *p53*$^{-/-}$ MEFs, which can be relieved by overexpression of E2F-1 or by blocking p16^{INK4A} function (Carnero et al. 2000). These data suggest that p19^{ARF} can target the pRB pathway independent of p53. The only known target of p19^{ARF} is MDM2, which can bind p53 but also pRB (Xiao et al. 1995) and may, thus, be a candidate to mediate the p19^{ARF}/pRB connection.

The role of pocket proteins in oncogenic transformation

Expression of so-called transforming oncogenes such as oncogenic RAS (Palmero et al. 1998) and v-Abl (Radfar et al. 1998) strongly increases the level of p19^{ARF}. This activates a p53-dependent checkpoint that protects cells from abnormal mitogenic signaling by inducing replicative arrest. MEFs lacking p19^{ARF} or p53 function are no longer susceptible to this type of protection; they escape from replicative senescence and become oncogenically transformed (Harvey and Levine 1991; Harvey et al. 1993; Kamijo et al. 1997). Overexpression of another

class of oncogenes such as MYC, adenovirus E1A, and E2F-1 in MEFs has been shown to enhance proliferation but also apoptosis (Lowe and Ruley 1993; Hermeking and Eick 1994; Wagner et al. 1994; Qin et al. 1994; Querido et al. 1997). Apoptosis is strongly enhanced by depriving cells of extracellular survival factors (Evan et al. 1992; Lowe and Ruley 1993) and is dependent on a functional p19^{ARF}-p53 pathway that does not involve p21^{CIP} function (Lowe et al. 1994; Wagner et al. 1994; Bates et al. 1998; De Stanchina et al. 1998; Zindy et al. 1998). The behavior of MYC- or E1A-expressing cells is highly reminiscent of that of triple-knockout cells: Pocket-protein ablation increased the proliferative capacity of cells but also their sensitivity to apoptosis: in particular, under conditions of low serum or high density. The picture that now emerges is that p19^{ARF} acts as a sensor of abnormal or conflicting mitogenic signaling, and activates a p53-dependent response that can either cause cell cycle arrest or sensitize cells to apotosis. The behavior of triple-knockout cells indicates that this decision depends on pocket-protein functions. In their presence, cells arrest; in their absence, for example, by genetic ablation, sequestration by E1A, or inhibition following overexpression of MYC (Berns et al. 2000; Lasorella et al. 2000), cells become immortal but also highly sensitive to apoptosis.

Indeed, we observed that culturing of triple-knockout MEFs under growth-restricting conditions readily induced apoptosis. At the same time, however, continuing cell proliferation was observed. Thus, under certain growth-restricting conditions, loss of pocket-protein function allows continuous cell turnover without net increase in cell number. We envisage that loss of pocket-protein function in vivo may also lead to increased cell turnover, which would strongly facilitate the acquisition of additional oncogenic events. Several observations lend support to this scenario. For example, conditional inactivation of *Rb* in the mouse pituitary gland resulted in increased cell turnover. Tumors appeared to arise from cells in which apoptosis was blocked, presumably through an additional mutation (Vooijs et al. 1997). Also, inactivation of the pRB family members in the mouse brain epithelium by the large T variant T121 induced aberrant proliferation and p53-dependent apoptosis. Inactivation of p53 in this setting resulted in a dramatic reduction in apoptosis (Yin et al. 1997). We speculate that redundancy of pocket proteins in cell cycle control is cell-type specific. For example, in the mouse pituitary gland, p107 and p130 may not be expressed or functional in compensating for loss of pRB, whereas in the mouse retina both pRB and p107 are active and, therefore, loss of both proteins is required to sustain prolonged cell turnover ultimately leading to retinoblastoma development (Robanus-Maandag et al. 1998).

In conclusion, we have identified three characteristics associated with loss of pocket-protein function that may provide a rationale for its frequent involvement in human cancer. These are reduced differentiation capacity, loss of the senescence response, and increased cell turnover under growth-restricting conditions. We expect that

a careful study of the fate of ES cells carrying single or compound loss-of-function mutations in the *Rb* gene family in chimeric mice will provide further insight into the role of pocket protein ablation in tumorigenesis.

Materials and methods

Generation of ES cells deficient for pRb, p107, and p130

Knockout alleles of *pRb*, *p107*, and *p130* were generated in 129Ola (E14/IB10) embryonic stem cells. The targeting vectors 129Rb-hyg, 129Rb-his, and 129p107-IRESβgeo have been described (te Riele et al. 1992; Robanus-Maandag et al. 1998). To inactivate *p130*, we generated the targeting construct 129p130-pur, in which a PGK-puromycin cassette was introduced into codon 405 residing in the A-domain of the pocket region (Le-Couter et al. 1996). On electroporation and selection at 1.8 µg/mL of puromycin, homologous recombinants were obtained with a frequency of 80%. The remaining allele of *p130* was inactivated by selection at high puromycin concentrations (14 µg/mL). *p130*$^{-/-}$ mice were generated using chimeric mice which gave germ-line transmission.

Generation of MEFs deficient for pRb, p107, and p130

Chimeric embryos were generated by injection of mutant ES cells into a 3.5-d-old C57Bl/6 blastocyst. Embryos we isolated 12 d after implantation and put into culture. Briefly, embryonic tissue without organs was washed in PBS, minced and incubated in 100 µL trypsin/EDTA overnight on ice and then 30 min at 37°C with an additional 100 µL of trypsin/EDTA. Mutant MEFs were selected for 48 h with 800 µg/mL G418. These cells were designated passage 1. Nonchimeric MEF cultures, serving as a control, all died within 48 h of selection.

ES cell culture, generation and characterization of teratocarcinomas

ES cells were cultured as described (Robanus-Maandag et al. 1998). Nude mice were injected subcutaneously with 10^6 ES cells. Tumors were removed 4 wk after injection, fixed in phosphate-buffered formalin, embedded in paraffin, sectioned at 5 µm, and stained with hematoxylin and eosin according to standard procedures. For immunohistochemical characterization, rehydrated sections were stained with antibodies against glial fibrillary acidic protein (GFAP, DAKO), low-affinity nerve growth factor receptor (p75^{LNGFR}, Chemicon International), neuron specific enolase (NSE, DAKO), and proliferation marker Ki-67 (MIB-5, Immunotech). The fraction of proliferating cells was determined by counting Ki-67-positive cells in six different areas in a teratocarcinoma section at a 160× magnification.

Culturing of MEFs, growth curves, 3T9 protocol

MEFs were cultured in GMEM (GIBCO) supplemented with 10% fetal calf serum, 1 mM nonessential amino acids, 1 mM sodium pyruvate, and 0.1 mM β-mercaptoethanol. For growth curves, MEFs were seeded at 2.5×10^4 cells per 12-well plate, in triplicate. At various time points, cells were washed with PBS, fixed for 5 min in 4% formaldehyde, and stained with 0.1% crystal violet (Sigma) in distilled water for 30 min. After washing the cells two times with water, they were allowed to dry. Staining was retrieved from the cells by adding 1 mL 10% acetic acid per well. Optical density was measured of 100 µL retrieved

staining at 590 nm. Values were normalized to the optical density at day 0.

A 3T9 protocol was performed by seeding 3×10^5 cells per 6-well plate, in triplicate. Cultures were incubated at 37°C for 3.5 d, and the total amount of cells was determined using a cell counter (Casy 1) followed by replating 3×10^5 cells. This protocol was repeated 20 times.

Electroporation of MEFs

MEFs were grown in 10-cm dishes to subconfluency. One to 2×10^6 cells were resuspended in 100 µL electroporation buffer (2 mM Hepes at pH 7.2, 15 mM K$_2$HPO$_4$/KH$_2$PO$_4$, 250 mM mannitol, and 1 mM MgCl$_2$) at 37°C. The cell suspension was mixed with plasmid DNA (histone H2B-GFP expression plasmid [Kanda et al. 1998], together with either a dominant-negative variant of CDK2 [Van den Heuvel and Harlow 1993] or pcDNA-*p19*^{Arf} in a 1 : 10 ratio) and transferred to an electroporation cuvette (0.1 cm, Biorad). After 5 min of incubation at room temperature, the cells were electroporated with Gene Pulser II/Gene Pulser II RF module apparatus (Biorad). Five minutes later, electroporation cells were taken up in 8 mL 37°C medium and seeded into a 10-cm dish. To measure effects on G$_1$, electroporated cells were blocked in G$_2$/M with nocodazole (0.5 µg/mL) 32 h after electroporation for 16 h. Cells were trypsinized and resuspended in 250 µL 0.1% Triton X-100 and 50 µg/mL propidium iodide in PBS. For each sample, 10.000 GFP-expressing cells were collected by FACS (FACscan, Becton Dickinson) and analyzed for their cell cycle distribution with the CellQuest program (Becton Dickinson).

FACS analysis

Cell cycle distribution of MEFs was determined by incubating MEFs with 5-Bromodeoxyuridine (0.3 µg/mL) plus 5-Fluoro-5-deoxyuridine (0.03 µg/mL) for 5 h. Cells were collected and resuspended in 70% alcohol at 4°C, stained with DAKO mouse anti-BrdU antibody, and prepared for FACS analysis as described in Brugarolas et al. (1995).

For cell size analysis, cultures were trypsinized, fixed in 70% alcohol at 4°C, stained with propidium iodide, and analyzed by FACS as described in Brugarolas et al. (1998).

Protein analysis

Protein levels were determined by Western blot analyses following established protocols. Antibodies against pRB (C-15), p107 (C-18), p130 (C-20), p16^{INK4A}(M-156), CDK4 (C-22), cyclin E (M-20), p21^{CIP} (C-19), and p53 (FL-393) were obtained from Santa Cruz; the p19^{ARF} antibody (R562) was obtained from Abcam. Goat antirabbit and goat antimouse secondary antibodies were from Biosource.

Irradiation of MEFs

After 5×10^5 cells were plated onto 10-cm dishes, tghey were irradiated the next day with 20 Gy of γ-radiation. Cell lysates were prepared after 24 h and analyzed on Western blots.

For cell cycle analysis, cells were irradiated with 5.5 Gy. After 14 h, cells were incubated with BrdU/FdU for 4 h and analyzed by FACS.

Soft agar assay

In GMEM containing 10% serum, 3×10^4 cells were resuspended in 2 mL 0.4% low–melting point agarose (Sigma) and

seeded, in duplicate, into six-well plates coated with 1% low–melting point agarose in GMEM containing 10% serum. The number of foci was scored after 2 wk.

References

Agarwal, M.L., Agarwal, A., Taylor, W.R., and Stark, G.R. 1995. p53 controls both the G2/M and the G1 cell cycle checkpoints and mediates reversible growth arrest in human fibroblasts. *Proc. Natl. Acad. Sci.* **92:** 8493–8497.

Bates, S., Phillips, A.C., Clark, P.A., Stott, F., Peters, G., Ludwig, R.L., and Vousden, K.H. 1998. p14ARF links the tumour suppressors RB and p53. *Nature* **395:** 124–125.

Bernards, R. 1997. E2F: A nodal point in cell cycle regulation. *Bichim. Biophys. Acta* **1333:** 33–40.

Berns, K., Martins, C., Dannenberg, J.-H., Berns, A., te Riele, H., and Bernards, R. 2000. p27kip-independent cell cycle regulation by MYC. *Oncogene* **19:** 4822–4827.

Brugarolas, J., Chandrasekaran, C., Gordon, J.I., Beach, D., Jacks, T., and Hannon, G.J. 1995. Radiation-induced cell cycle arrest compromised by p21 deficiency. *Nature* **377:** 552–557.

Brugarolas, J., Bronson, R.T., and Jacks, T. 1998. p21 is a critical CDK2 regulator essential for proliferation control in *Rb*-deficient cells. *J. Cell Biol.* **141:** 503–514.

Campisi, J. 1997. The biology of replicative senescence. *Eur. J. Cancer* **33:** 703–709.

Carnero, A., Hudson, J.D., Price, C.M., and Beach, D.H. 2000. p16^INK4A and p19^ARF act in overlapping pathways in cellular immortalization. *Nat. Cell Biol.* **2:** 148–155.

Clarke, A.R., Robanus Maandag, E., Van Roon, M., Van der Lugt, N.M.T., Van der Valk, M., Hooper, M.L., Berns, A., and te Riele, H. 1992. Requirement for a functional Rb-1 gene in murine development. *Nature* **359:** 328–330.

Cobrinik, D., Lee, M.-H., Hannon, G., Mulligan, G., Bronson, R.T., Dyson, N., Harlow, E., Beach, D., Weinberg, R.A., and Jacks, T. 1996. Shared role of the pRB-related p130 and p107 proteins in limb development. *Genes* & *Dev.* **10:** 1633–16344.

DeCaprio, J.A., Ludlow, J.W., Figge, J., Shew, J.-Y., Huang, C.-M., Lee, W.-H., Marsilio E., Paucha, E., and Livingston, D.M. 1988. SV40 large tumor antigen forms a specific complex with the product of the retinoblastoma susceptibility gene. *Cell* **54:** 275–283.

De Stanchina, E., McCurrach, M.E., Zindy, F., Shieh, S.Y., Ferbeyre, G., Samuelson, A.V., Prives, C., Roussel, M.F., Sherr, C.J., and Lowe, S.W. 1998. E1A signaling to p53 involves the p19(ARF) tumor suppressor. *Genes* & *Dev.* **12:** 2434–2442.

Dyson, N. 1998. The regulation of E2F by pRB-family proteins. *Genes* & *Dev.* **12:** 2245–2262.

Dyson, N., Howley, P.M., Munger, K., and Harlow, E. 1989. The human papillomavirus-16 E7 oncoprotein is able to bind to the retinoblastoma gene product. *Science* **243:** 934–936.

Evan, G.I., Wyllie, A.H., Gilbert, C.S., Littlewood, T.D., Land, H., Brooks, M., Waters, C., Penn, L.Z., and Hancock, D.C. 1992. Induction of apoptosis in fibroblasts by c-myc protein. *Cell* **69:** 119–128.

Fang, F., Orend, G., Watanabe, N., Hunter, T., and Ruoslahti, E. 1996. Dependence of cyclin E-CDK2 kinase activity on cell anchorage. *Science* **271:** 499–502.

Friedrich, G. and Soriano, P. 1991. Promoter traps in embryonic stem cells: A genetic screen to identify and mutate developmental genes in mice. *Genes* & *Dev.* **5:** 1513–1523.

Groth, A., Weber, J.D., Willumsen, B.M., Sherr, C.J., and Roussel, M.F. 2000. Oncogenic Ras induces p19^ARF and growth arrest in mouse embryo fibroblasts lacking p21^Cip1 and p27Kip1 without activating cyclin D-dependent kinases. *J. Biol. Chem.* **275:** 27473–27480.

Guadagno, T.M., Ohtsubo, M., Roberts, J.M., and Assoian, R.K. 1993. A link between cyclin A expression and adhesion-dependent cell cycle progression. *Science* **262:** 1572–1575.

Hall, M. and Peters, G. 1996. Genetic alterations of cyclins, cyclin-dependent kinases, and Cdk inhibitors in human cancer. *Adv. Cancer Res.* **68:** 67–108.

Harbour, J.W., Lai, S.-L., Whang-Peng, J., Gazdar, A.F., Minna, J.D., and Kaye, F.J. 1988. Abnormalities in structure and expression of the human retinoblastoma gene in SCLC. *Science* **241:** 353–357.

Harrington, E.A., Bruce, J.L., Harlow, E., and Dyson, N. 1998. pRB plays an essential role in cell cycle arrest induced by DNA damage. *Proc. Natl. Acad. Sci.* **95:** 11945–11950.

Harvey, D.M. and Levine, A.J. 1991. p53 alteration is a common event in the spontaneous immortalization of primary BALB/c murine fibroblasts. *Genes* & *Dev.* **5:** 2375–2385.

Harvey, M., Sands, A.T., Weiss, R.S., Hegi, M.E., Wiseman, R.W., Pantazis, P., Giovanella, B.C., Tainsky, M.A., Bradley, A., and Donehower, L.A. 1993. In vitro growth characteristics of embryo fibroblasts isolated of p53-deficient mice. *Oncogene* **8:** 2547–2467.

Hayflick, L. and Moorhead, P.S. 1961. The serial cultivation of human diploid cell strains. *Exp. Cell Res.* **25:** 585–621.

Hermeking, H. and Eick, D. 1994. Mediation of c-Myc-induced apoptosis by p53. *Science* **265:** 2091–2093.

Herrera, R.E., Sah, V.P., Williams, B.O., Weinberg, R.A., and Jacks, T. 1996. Altered cell cycle kinetics, gene expression and G1 restriction point regulation in Rb-deficient fibroblasts. *Mol. Cell. Biol.* **16:** 2402–2407.

Horowitz, J.M., Park, S.-H., Bogenmann, E., Cheng J.-C., Yandell, D.W., Kaye, F.J., Minna, J.D., Drya, T.P. and Weinberg, R.A. 1990. Frequent inactivation of the retinoblastoma anti-oncogene is restricted to a subset of human tumor cells. *Proc. Natl. Acad. Sci.* **87:** 2775–2779.

Hu, N., Gutsmann, A., Herbert, D.C., Bradley, A., Lee, W.-H., and Lee, E.Y.-H.P. 1994. Heterozygous *Rb-1Δ20/+* mice are predisposed to tumors of the pituitary gland with a nearly complete penetrance. *Oncogene* **9:** 1021–1027.

Hurford, R.K., Cobrinik, D., Lee, M.-H., and Dyson, N. 1997. pRB and p107/p130 are required for the regulated expression of different sets of E2F responsive genes. *Genes* & *Dev.*

11: 1447–1463.

Jacks, T., Fazeli, A., Schmitt, E.M., Bronson, R.T., Goodell, M.A., and Weinberg, R.A. 1992. Effects of an Rb mutation in the mouse. *Nature* **359:** 295–300.

Kamb, A., Gruis, N.A., Weaver-Feldhaus, J., Liu, Q., Harshman, K., Tavtigian, S.V., Stockert, E., Day III, R.S., Johnson, B.E., and Skolnick, M.H. 1994. A cell cycle regulator involved in genesis of many tumor types. *Science* **264:** 436–440.

Kamijo, T., Zindy, F., Roussel, M.F., Quelle, D.E., Downing, J.R., Ashmun, R.A., Grosveld, G., and Sherr, C.J. 1997. Tumor suppresion at the mouse INK4a locus mediated by the alternative reading frame product p19arf. *Cell* **91:** 649–659.

Kamijo, T., Weber, J.D., Zambetti, G., Zindy, F., Roussel, M.F., and Sherr, C.J. 1998. Functional and physical interactions of the ARF tumor suppressor with p53 and Mdm2. *Proc. Natl. Acad. Sci.* **95:** 8292–8287.

Kanda, T., Sullivan, K.F., and Wahl, G.M. 1998. Histone-GFP fusion protein enables sensitive analysis of chromosome dynamics in living mammalian cells. *Curr. Biol.* **8:** 377–385.

Lasorella, A., Noseda, M., Beyna, M., and Iavarone, A. 2000. Id2 is a retinoblastoma protein target and mediates signalling by Myc oncoproteins. *Nature* **407:** 592–598.

LeCouter, J.E., Whyte, P.F., and Rudnicki, M.A. 1996. Cloning and expression of the Rb-related mouse p130 mRNA. *Oncogene* **12:** 1433–1440.

LeCouter, J., Kablar, B., Hardy, W.R., Ying, C., Megeney, L.A., May, L.L., and Rudnicki, M.A. 1998a. Strain-dependent myeloid hyperplasia, growth deficiency and accelerated cell cycle in mice lacking the Rb-related *p107* gene. *Mol. Cell. Biol.* **18:** 7455–7465.

LeCouter, J., Kablar, B., Whyte, P.F.M., Ying, C., and Rudnicki, M.A. 1998b. Strain-dependent embryonic lethality in mice lacking the retinoblastoma-related p130 gene. *Development* **125:** 4669–4679.

Lee, E.Y.-H.P., To, H., Shew J.-Y., Bookstein, R., Scully, P., and Lee, W.-H. 1988. Inactivation of the retinoblastoma susceptibility gene in human breast cancers. *Science* **241:** 218–221.

Lee, E.Y.-H.P., Chang, C.-Y., Hu, N., Wang, Y.-C., Lai, C.-C., Herrup, K., Lee, W.-H., and Bradley, A. 1992. Mice deficient for Rb are nonviable and show defects in neurogenesis and haematopoiesis. *Nature* **359:** 288–294.

Lee, M.-H., Williams, B.O., Mulligan, G., Mukai, S., Bronson, R.T., Dyson, N., Harlow, E., and Jacks, T. 1996. Targeted disruption of *p107*: Functional overlap between *p107* and *Rb*. *Genes & Dev.* **10:** 1621–1632.

Lipinski, M.M. and Jacks, T. 1999. The retinoblastoma gene family in differentiation and development. *Oncogene* **18:** 7873–7882.

Lloyd, A.C., Obermuller, F., Staddon, S., Barth, C.F., McMahon, M., and Land, H. 1997. Cooperating oncogenes converge to regulate cyclin/cdk complexes. *Genes & Dev.* **11:** 663–677.

Lowe, S.W. and Ruley, H.E. 1993. Stabilization of the p53 tumor suppressor is induced by adenovirus 5 E1A and accompanies apoptosis. *Genes & Dev.* **7:** 535–545.

Lowe, S.W., Jacks, T., Housman, D.E., and Ruley, H.E. 1994. Abrogation of oncogene-associated apoptosis allows transformation of p53-deficient cells. *Proc. Natl. Acad. Sci.* **91:** 2026–2030.

Morgenbesser, S.D., Williams, B.O., Jacks, T., and DePinho, R.A. 1994. p53-dependent apoptosis produced by *Rb*-deficiency in the developing mouse lens. *Nature* **371:** 72–74.

Mulligan, G. and Jacks, T. 1998. The retinoblastoma gene family: Cousins with overlapping interests. *Trends Genet.* **14:** 223–229.

Mulligan, G.J., Wong, J., and Jacks, T. 1998. p130 is dispensable in peripheral T lymphocytes: Evidence for functional compensation by p107 and pRB. *Mol. Cell. Biol.* **18:** 206–220.

Murray, E.J., Stott, D., and Rigby, P.W.J. 1991. Sequences and factors required for the F9 embryonal carcinoma stem cell E1a-like activty. *Mol. Cell. Biol.* **11:** 5534–5540.

Nevins, J.R. 1998. Toward an understanding of the functional complexity of the E2F and retinoblastoma families. *Cell Growth Diff.* **9:** 585–593.

Nilausen, K. and Green, H. 1965. Reversible arrest of growth in G1 of an established cell fibroblast line (3T3). *Exp. Cell Res.* **40:** 166–168.

Nobori, T., Miura, K., Wu, D.J., Lois, A., Tkbayashi, K., and Carson, D.A. 1994. Deletions of the cyclin-dependent kinase-4 inhibitor gene in multiple human cancers. *Nature* **368:** 753–756.

Ohtsubo, M. and Roberts, J.M. 1993. Cyclin-dependent regulation of G1 in mammalian fibroblasts. *Science* **259:** 1908–1912.

Palmero, I., McConnell, B., Parry, D., Brookes, S., Hara, E., Bates, S., Jat, P., and Peters, G. 1997. Accumulation of p16INK4a in mouse fibroblasts as a function of replicative senescence and not of retinoblastoma gene status. *Oncogene* **15:** 495–503.

Palmero, I., Pantoja, C., and Serrano, M. 1998. p19^{ARF} links the tumour suppressor p53 to Ras. *Nature* **395:** 125–126.

Pantoja, C. and Serrano, M. 1999. Murine fibroblasts lacking p21 undergo senescence and are resistant to transformation by oncogenic Ras. *Oncogene* **18:** 4974–4982.

Polyak, K., Kato, J.Y., Solomon, M.J., Sherr, C.J., Massague, J., Roberts, J.M., and Koff, A. 1994. p27Kip, a cyclin-cdk inhibitor, links transforming growth factor-β and contact inhibition to cell cycle arrest. *Genes & Dev.* **8:** 9–22.

Pomerantz, J., Schreiber-Agus, N., Liegeois, N.J., Silverman, A., Alland, L., Chin, L., Potes, J., Chen, K., Orlow, I., Lee, H.W., et al. 1998. The Ink4a tumor suppressor gene product, p19^{Arf}, interacts with MDM2 and neutralizes MDM2's inhibition of p53. *Cell* **92:** 713–723.

Qin, X.-Q., Livingston, D.M., Kaelin, W.G., and Adams, P.D. 1994. Deregulated transcription factor E2F-1 expression leads to S-phase entry and p53-mediated apoptosis. *Proc. Natl. Acad. Sci.* **91:** 10918–10922.

Quelle, D.E., Zindy, F., Ashmun, R.A., and Sherr, C.J. 1995. Alternative reading frames of the INK4a tumor suppressor gene encode two unrelated proteins capable of inducing cell cycle arrest. *Cell* **83:** 993–1000.

Querido, E., Teodoro, J.G., and Branton, P.E. 1997. Accumulation of p53 induced by the adenovirus E1A protein requires regions involved in the stimulation of DNA synthesis. *J. Virol.* **71:** 3526–3533.

Radfar, A., Unnikrishnan, I., Lee, H.W., DePinho, R.A., and Rosenberg, N. 1998. p19(Arf) induces p53-dependent apoptosis during abelson virus-mediated pre-B cell transformation. *Proc. Natl. Acad. Sci.* **95:** 13194–13197.

Rittling, S.R. and Denhardt, D.T. 1992. p53 mutations in spontaneously immortalized 3T12 but not 3T3 mouse embryo cells. *Oncogene* **7:** 935–942.

Robanus-Maandag, E.C., Van der Valk, M., Vlaar, M., Feltkamp, C., O'Brien, J., Van Roon, M., Van der Lugt, N., Berns, A., and te Riele, H. 1994. Developmental rescue of an embryonic-lethal mutation in the retinoblastoma gene in chimeric mice. *EMBO J.* **13:** 4260–4268.

Robanus-Maandag, E., Dekker, M., Van der Valk, M., Carrozza, M.-L., Jeanny, J.-C., Dannenberg, J.-H., Berns, A., and te Riele, H. 1998. p107 is a suppressor of retinoblastoma development in pRb-deficient mice. *Genes & Dev.* **12:** 1599–1609.

Savatier, P., Huang, S., Szekely, L., Wiman, K.G., and Samarut, J. 1994. Contrasting patterns of retinoblastoma protein ex-

pression in mouse embryonic stem cells and embryonic fibroblasts. *Oncogene* **9:** 809–818.

Savatier, P., Lapillonne, H., van Grunsven, L.A., Rudkin, B.B., and Samarut, J. 1996. Withdrawal of differentiation inhibitory activity/leukemia inhibitory factor up-regulates D-type cyclins and cyclin-dependent kinase inhibitors in mouse embryonic stem cells. *Oncogene* **18:** 309–322.

Schulze, A., Zerfass-Thome, K., Bergès, J., Middendorp, S., Jansen-Dürr, P., and Henglein, B. 1996. Anchorage-dependent transcription of the cyclin A gene. *Mol. Cell. Biol.* **16:** 4632–4638.

Serrano, M., Hannon, G.J., and Beach, D. 1993. A new regulatory motif in cell-cycle control causing specific inhibition of cyclin D/CDK4. *Nature* **366:** 704–707.

Serrano, M., Lee, H.-W., Chin, L., Cordon-Cardo, C., Beach, D., and DePinho, R.A. 1996. Role of the INK4a locus in tumor suppression and cell mortality. *Cell* **85:** 27–37.

Serrano, M., Lin, A.W., Mila, E.M., Beach, D., and Lowe, S.W. 1997. Oncogenic ras provokes premature cell senescence associated with accumulation of p53 and p16$^{\text{ink4a}}$. *Cell* **88:** 593–602

Sherr, C.J. 1996 Cancer cell cycles. *Science* **274:** 1672–1677.

St. Croix, B., Sheehan, C., Rak, J.W., Florenes, V.A., Slingerland, J.M., and Kerbel, R.S. 1998. E-cadherin-dependent growth suppression is mediated by the cyclin-dependent kinase inhibitor p27(KIP1) *J. Cell. Biol.* **142:** 557–571.

Te Riele, H., Robanus-Maandag, E., and Berns, A. 1992. Highly efficient gene targeting in embryonic stem cells through homologous recombination with isogenic DNA constructs. *Proc. Natl. Acad. Sci.* **89:** 5128–5132.

Todaro, G.J. and Green, H. 1963. Quantitative studies of the growth of mouse embryo cells in culture and their development into established lines. *J. Cell Biol.* **17:** 299–313.

Tsai, K.Y., Hu, Y., Macleod, K.F., Crowley, D., Yamasaki, L., and Jacks, T. 1998. Mutation of *E2f-1* suppresses apoptosis and inappropiate S phase entry and extends survival of *Rb*-deficient mouse embryos. *Mol. Cell* **2:** 293–304.

Van den Heuvel, S. and Harlow, E. 1993. Distinct roles for cyclin-dependent kinases in cell cycle control. *Science* **262:** 2050–2054.

Vooijs, M., van der Valk, M., te Riele, H., and Berns, A. 1998. Flp-mediated tissue-specific inactivation of the retinoblastoma tumor suppressor gene in the mouse. *Oncogene* **17:** 1–12.

Wagner, A.J., Kokontis, J.M., and Hay, N. 1994. Myc-mediated apoptosis requires wild-type p53 in a manner independent of cell cycle arrest and the ability of p53 to induce p21waf1/cip1. *Genes & Dev.* **8:** 2817–2830.

Weinberg, R.A. 1995. The retinoblastoma protein and cell cycle control. *Cell* **81:** 323–330.

Whyte, P., Buchkovich K.J., Horowitz, J.M., Friend, S.H., Raybuck, M., Weinberg, R.A., and Harlow, E. 1988. Association between an oncogene and an anti-oncogene: The adenovirus E1A proteins bind to the retinoblastoma gene product. *Nature* **334:** 124–129.

Xiao, Z.X., Chen, J., Levine, A.J., Modjtahedi, N., Xing, J., Sellers W.R., and Livingston, D.M. 1995. Interaction between the retinoblastoma protein and the oncoprotein MDM2. *Nature* **375:** 694–698.

Yin, C., Knudson, C.M., Korsmeyers, J.S., and Van Dyke, T. 1997. Bax suppresses tumorigenesis and stimulates apoptosis in vivo. *Nature* **385:** 637–640.

Zhang, H.S., Postigo, A.A., and Dean, D.C. 1999. Active transcriptional repression by the Rb-E2F complex mediates G1 arrest triggered by p16$^{\text{INK4A}}$, TGFβ, and contact inhibiton. *Cell* **97:** 53–61.

Zhang, S., Ramsay, E.S., and Mock, B. 1998. *Cdkn2a*, the cyclin-dependent kinase inhibitor encoding p16INK4a and p19$^{\text{ARF}}$, is a candidate for the plasmacytoma susceptibility locus, *Pctr1*. *Proc. Natl. Acad. Sci.* **95:** 2429–2434.

Zhang, Y., Xiong, Y., and Yarbrough, W.G. 1998. ARF promotes MDM2 degradation and stabilizes p53: ARF-INK4a locus deletion impairs both the Rb and p53 tumor suppression pathways. *Cell* **92:** 725–734.

Zindy, F., Quelle, D.E., Roussel, M.F., and Sherr, C.J. 1997. Expression of the p16INK4a tumor suppressor versus other INK4 family members during mouse development and aging. *Oncogene* **15:** 203–211.

Zindy, F., Eischen, C.M., Randle, D., Kamijo, T., Cleveland, J.L., Sherr, C.J., and Roussel, M.F. 1998. Myc signaling via the ARF tumor suppressor regulates p53-dependent apoptosis and immortalization. *Genes & Dev.* **12:** 2424–2433.

Zorick, T.S. and Lemke, G. 1996. Schwann cell differentiation. *Curr. Opin. Cell Biol.* **8:** 870–876.